Acta Mechanica 77, 281—297 (1989)

ACTA MECHANICA

Adiabatic Shear Banding in a Bimetallic Body

By

R. C. Batra and **Y. W. Kwon**, Rolla, Missouri

With 8 Figures

(*Received May 5, 1988; revised September 14, 1988*)

Summary

Thermomechanical deformations of a body made of two different materials and undergoing simple shearing deformations are studied with the objectives of finding out when and where adiabatic shear bands will initiate and how they will subsequently grow. Each material is modeled as strain and strain-rate hardening but thermally softening. A shear band is presumed to have formed if the introduction of a temperature perturbation centered around the common interface between the two materials results in an eventual localization of the deformation into a region of width considerably smaller than the width of the initial temperature bump. For a fixed set of material properties the effect of the applied overall strain-rate, and for a fixed applied strain-rate the effect of varying the shear modulus, thermal conductivity, and the coefficient of thermal softening of one material relative to the other have been examined. It is found that a shear band forms in the material that softens more rapidly.

1. Introduction

Adiabatic shear banding is the name given to a localization phenomenon that occurs in high strain-rate plastic deformation, such as machining, metal forming, and ballistic penetration. Practical interest in the phenomenon derives from the fact that once a shear band has formed, most of the subsequent deformations occur in the narrow region of the band and the load carrying capacity of the body is severely impaired. These shear bands are often precursors to shear fractures.

Since the time Zener and Hollomon [1] observed shear bands in a steel plate punched by a standard die and postulated that a negative slope of the stress-strain curve implies an intrinsic instability of the material, there have been many analytical (e.g. Recht [2], Staker [3], Clifton [4], Clifton and Molinari [5], Burns [6], Wright [7], Anand et al. [8], Bai [9], Coleman and Hodgdon [10]), experimental (e.g. Moss [11], Costin et al. [12], Marchand and Duffy [13]) and numerical (e.g. Clifton et al. [14], Merzer [15], Wu and Freund [16], Wright and Batra [17], [18], Wright and Walter [19], Batra [20]–[22]) studies aimed at understanding the factors that enhance or inhibit the shear strain localization. Rogers [23], [24] has elegantly summarized in his review articles the works dealing with adiabatic shear banding that were completed until 1982. All of the works enumerated above have studied adiabatic shear banding in monolithic materials. In some of the analytical and all of the numerical works, a material inhomogeneity/flaw has been modeled by introducing a perturbation, say in the temperature field, and studying the subsequent growth of all of the field variables.

Here we study the initiation and growth of adiabatic shear bands in a body made of two different materials and undergoing simple shearing deformations. The material of each layer exhibits strain and strain-rate hardening and thermal softening. A temperature perturbation symmetrical about the common interface is introduced and the body is presumed to be placed in a hard loading device in the sense that the velocity of points on the end faces is prescribed. The resulting nonlinear initial-boundary-value problem has been solved numerically by the Crank-Nicolson-Galerkin method. In every case studied, the deformation is found to localize completely within the material for which the peak value of the shear stress occurs at a lower value of the average shear strain.

2. Formulation of the Problem

We study thermomechanical deformations of a bimetallic body undergoing simple shearing motion. With respect to a rectangular Cartesian set of axes, the deformations of the body are assumed to be given by

$$x = X + u(Y, t), \qquad y = Y, \qquad z = Z, \qquad \theta = \theta(Y, t) \tag{1}$$

where (x, y, z) is the current position of a material particle that occupied the place (X, Y, Z) in the stress free reference configuration, θ denotes the temperature change and u gives the x-displacement of a material particle. The deformations of material points that are not on the common interface between the two materials are governed by

$$\varrho \dot{v} = s_{,y} \tag{2.1}$$

$$\varrho \dot{e} = -q_{,y} + s v_{,y}, \tag{2.2}$$

where $v = \dot{x}$ is the x-velocity of a material particle, s is the shear stress, q is the heat flux in the y-direction, a superimposed dot indicates material time differentiation, and a comma followed by y implies partial differentiation with respect to y. Equations (2.1) and (2.2) express, respectively, the balance of linear momentum and the balance of internal energy. We presume that the strain rate has an additive decomposition into elastic $\dot{\gamma}_e$ and plastic parts $\dot{\gamma}_p$, i.e.,

$$\dot{\gamma} = v_{,y} = \dot{\gamma}_e + \dot{\gamma}_p . \tag{3}$$

For the constitutive relations we take

$$\dot{s} = \mu \dot{\gamma}_e , \tag{4.1}$$

$$q = -k\theta_{,y} , \tag{4.2}$$

$$e = c\theta + \frac{1}{2}\frac{\mu}{\varrho}\gamma_e^2 , \tag{4.3}$$

$$\dot{\gamma}_p = \Lambda s , \qquad \Lambda \begin{cases} = 0 \text{ for elastic deformations,} \\ > 0 \text{ for plastic deformations.} \end{cases} \tag{4.4}$$

Here μ is the shear modulus, k the thermal conductivity, and c the specific heat. A material point is presumed to undergo plastic deformations if at that point

$$f(s, \theta, \dot{\gamma}_p) > \varkappa , \tag{5}$$

where f is the yield function and $\varkappa$ describes the work hardening of the material. The thermal softening and strain-rate hardening characteristics of the material are embodied into f by requiring that

$$\frac{\partial f}{\partial \theta} > 0 \quad \text{and} \quad \frac{\partial f}{\partial \dot{\gamma}_p} < 0 . \tag{6}$$

We presume that

$$f(s, \theta, \dot{\gamma}_p) = s/[(1 - a\theta)(1 + b\dot{\gamma}_p)^m] , \tag{7.1}$$

$$\varkappa = \varkappa_0 (1 + \psi/\psi_0)^n , \tag{7.2}$$

$$\varkappa \dot{\psi} = s\dot{\gamma}_p , \tag{7.3}$$

where a, b, m, n, and ψ_0 are material constants and $\varkappa_0$ is the yield stress of the material in a quasi-static isothermal simple shearing test. Equation (7.3) specifies the rate of evolution of the work-hardening parameter ψ. Equations (4.4), (5), (7.1) and (7.2) imply that a material point is deforming elastically if

$$s \leqq \varkappa_0 \left(1 + \frac{\psi}{\psi_0}\right)^n (1 - a\theta) . \tag{8}$$

For elasto-plastic deformations of the material point, the plastic strain-rate $\dot{\gamma}_p$ satisfies

$$s = \varkappa_0 \left(1 + \frac{\psi}{\psi_0}\right)^n (1 - a\theta)(1 + b\dot{\gamma}_p)^m . \tag{9}$$

The constitutive relation (9) is a slight generalization of that proposed by Litonski [25] and has been used by Burns [6], Wright and Batra [17], [18], and Batra [20], [21]. Substitution from Eqs. (3), (4.1), (4.2) and (4.3) into Eq. (2.2) gives

$$\varrho c\dot{\theta} = k\theta_{,yy} + s\dot{\gamma}_p \,. \tag{10}$$

Thus all of the plastic working is presumed to be converted into heat. We note that Farren and Taylor [26] found that in tensile experiments on steels, copper and aluminum, the heat rise represented 86.5, 90.5—92, and 95%, respectively, of the plastic work.

At points on the interface $y = 0$ between the two materials,

$$[s] = 0, \qquad [v] = 0, \tag{11.1}$$

$$[q] = 0, \qquad [\theta] = 0, \tag{11.2}$$

where $[s]$ denotes the difference in the limiting values of s as the point on the common interface is approached from the two sides. Thus Eqs. (11.1) and (11.2) ensure the continuity of the shear stress and the heat flux across the interface between the two constituents of the body.

We consider the case when the body is placed in an insulated hard loading device and accordingly impose the following conditions on its top $Y = H$ and bottom $y = -H$ faces.

$$\begin{aligned} v &= \pm v_0 \quad \text{at} \quad y = \pm H, \\ q &= 0 \quad \text{at} \quad y = \pm H. \end{aligned} \tag{12}$$

For the initial conditions we take

$$\begin{gathered} v(y, 0) = y, \qquad \psi(y, 0) = 0, \qquad \theta(y, 0) = 0.1(1 - y^2)^9 \, e^{-5y^2}, \\ s(y, 0) = \varkappa_0\big(1 - a\theta(y, 0)\big). \end{gathered} \tag{13}$$

Thus initially each material point is assumed to lie on its yield surface that corresponds to its prescribed temperature and zero plastic strain-rate.

3. Computation and Discussion of Results

Batra [20] has given the details of the Crank-Nicolson-Galerkin method used to integrate Eqs. (2) and (4) subject to the boundary conditions (12) and initial conditions (13). That computer code based on the non-dimensional form of the equations, was modified to use the present dimensional form of equations. The advantage of using the dimensional form of equations is that the continuity conditions (11) are easily built into the Galerkin formulation of the problem. The domain $[-H, +H]$ was divided into 400 uniform elements (cf. Fig. 1a)

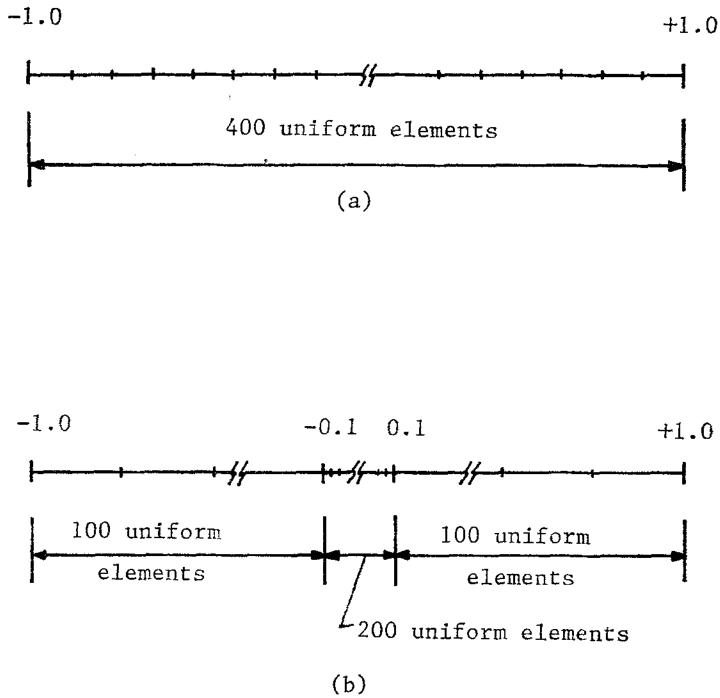

Fig. 1. Finite element meshes used

and the time increment $\Delta t = 5 \times 10^{-6} H/v_0$ was used to integrate the governing equations.

We first list the values of material and geometric parameters that were assigned the same values for both constituents of the body.

$$H = 2.58\ \mathrm{mm}, \qquad \varrho = 7{,}860\ \mathrm{kg\,m^{-3}}, \qquad \varkappa_0 = 333\ \mathrm{MPa},$$
$$c = 473\ \mathrm{J\,kg^{-1}\,{}^\circ C^{-1}},$$
$$m = 0.0245, \qquad n = 0.09, \qquad \psi_0 = 0.017, \qquad b = 10^4\ \mathrm{sec};$$

The material properties of the body occupying the region $[0, H]$ are labeled by subscript 2 and that of the other part of the body by subscript 1. For material 1 we took:

$$\mu_1 = 80\ \mathrm{GPa}, \qquad k_1 = 49.216\ \mathrm{W\,m^{-1}\,{}^\circ C^{-1}}, \qquad a_1 = 0.00552\ {}^\circ\mathrm{C}^{-1},$$

and studied the effect of varying the properties of material 2. The chosen values of parameters for material 1 are for a typical hard steel, except that the value of the thermal softening coefficient a is nearly seven times what it ought to be. This is done to reduce the computational time needed to solve the problem, and should not affect the results qualitatively. In the first set of numerical experiments, the overall applied strain-rate was kept fixed at $500\ \mathrm{sec}^{-1}$ and only one out of three variables μ, k and a was changed. In the second set of computations, the effect of changing the average strain-rate to 5,000 $\sec^{-1}$ and 50,000 $\sec^{-1}$ for a fixed set of material properties was analyzed.

To ensure that the computer code had been correctly changed, we solved the problem for a homogeneous body studied earlier by Batra [20]. For the test problem, results identical to those computed previously were obtained. Subsequently we set $\mu_2/\mu_1 = 0.9$, $k_2/k_1 = 1.0$, $a_2/a_1 = 1.0$ and then $\mu_2/\mu_1 = 1.0$, $k_2/k_1 = 0.8$ and $a_2/a_1 = 1.0$ but did not introduce any temperature perturbation. There was no localization of the deformation observed in either case.

Before discussing the computed results we note that the emphasis here is to see where the band forms and its possible shape. Batra [21], [22] has studied the effect of various material parameters and the applied strain-rate on the initiation and growth of a shear band in a homogeneous body. In keeping with the aforementioned objective the variation of the field variables within the domain $(-0.1H, +0.1H)$ is plotted. We first discuss results when the prescribed velocity at the top and bottom faces is kept fixed at ± 1.20 m/sec. This corresponds to an average strain-rate of 500 $\sec^{-1}$.

Figures 2 and 3 show the variations of the temperature, plastic strain-rate and the particle velocity within the specimen at two different times and for four different values of a_2/a_1. Soon after (see Fig. 2) the symmetric temperature perturbation is introduced, the temperature becomes nonsymmetrical about the centerline. This asymmetry is more pronounced for $a_2/a_1 = 0.5$ and 1.2 as compared to that for $a_2/a_1 = 0.8$ and 0.9. Also the velocity gradient is discontinuous at the center. The plastic strain-rate is also nonsymmetrical about the centerline and follows a pattern somewhat akin to that of the temperature except that it exhibits oscillatory behavior near the centerline.

The plastic strain-rate at the center suffers a jump because the shear stress becomes essentially uniform throughout the specimen soon after the temperature perturbation is introduced and stays uniform until the time results are presented here. Since the temperature is continuous across the centerline, the higher value of the thermal softening coefficient a lowers the flow stress for the material point $y = 0^-$ as compared to that at $y = 0^+$ if $a_2/a_1 < 1.0$. According to our constitutive assumptions the plastic strain-rate at a point is proportional to the amount by which the stress at the point exceeds the flow stress. Thus the plastic strain-rate at the point $y = 0^-$ should exceed that at the point $y = 0^+$ if $a_2/a_1 < 1.0$.

The values of γ_{avg} or the time when the deformation seems to have localized is different for the four cases (see Fig. 3). For $a_2/a_1 = 1.0$, the deformation localized when $\gamma_{\text{avg}} = 0.0745$. For all four values of a_2/a_1 the shear band formed within the material having the higher value of the thermal softening coefficient. For $a_2/a_1 = 0.5, 0.8, 0.9$, and 1.2, the peak plastic strain-rate occurred at $y/H = -0.0040$, -0.035, -0.030, and $+0.030$, respectively. Thus the higher the difference between the values of a_2 and a_1, the larger the shift of the center of the band away from the center of the specimen. Note that for every value of a_2/a_1 considered herein,

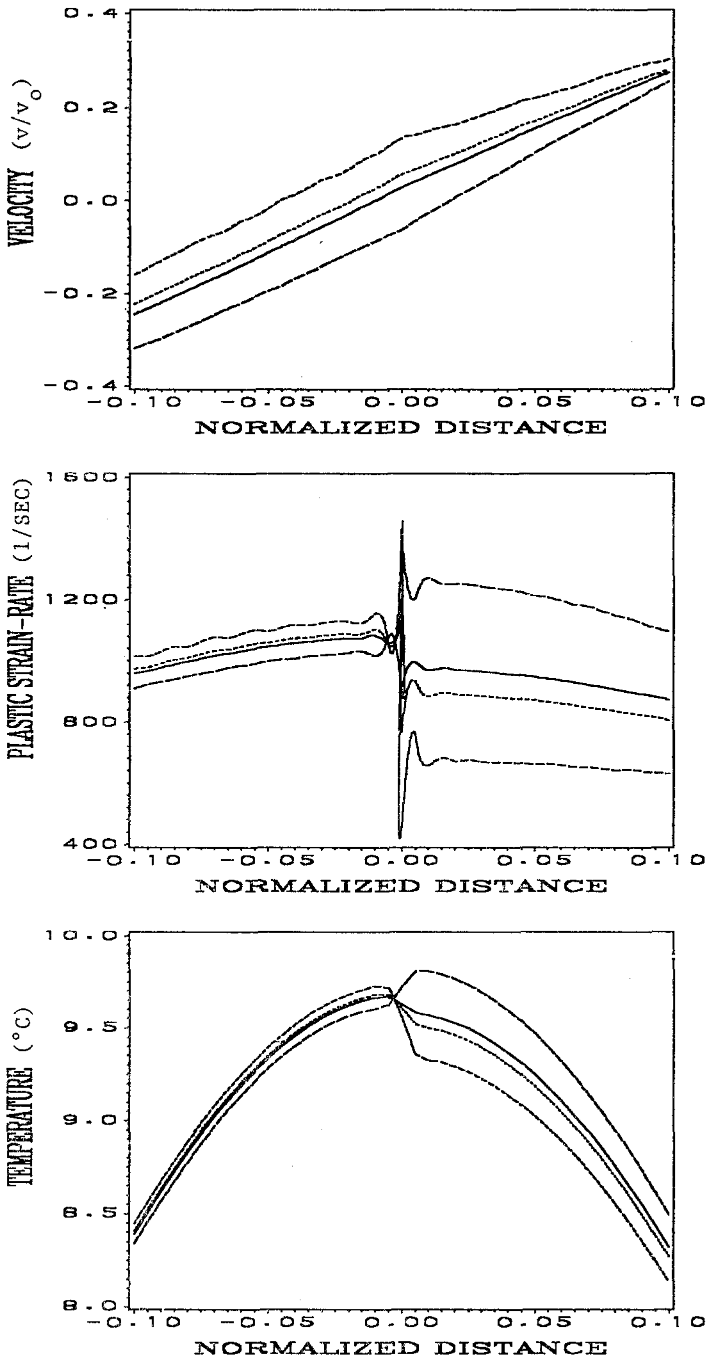

Fig. 2. Distribution of the particle velocity, plastic strain-rate and temperature for $a_2/a_1 = 0.5$, 0.8, 0.9, 1.2 and $\dot{\gamma}_0 = 500\ \text{sec}^{-1}$ at $\gamma_{avg} = 0.004$. (------ $a_2/a_1 = 0.5$; ······ $a_2/a_1 = 0.8$; ——— $a_2/a_1 = 0.9$; — — — $a_2/a_1 = 1.2$)

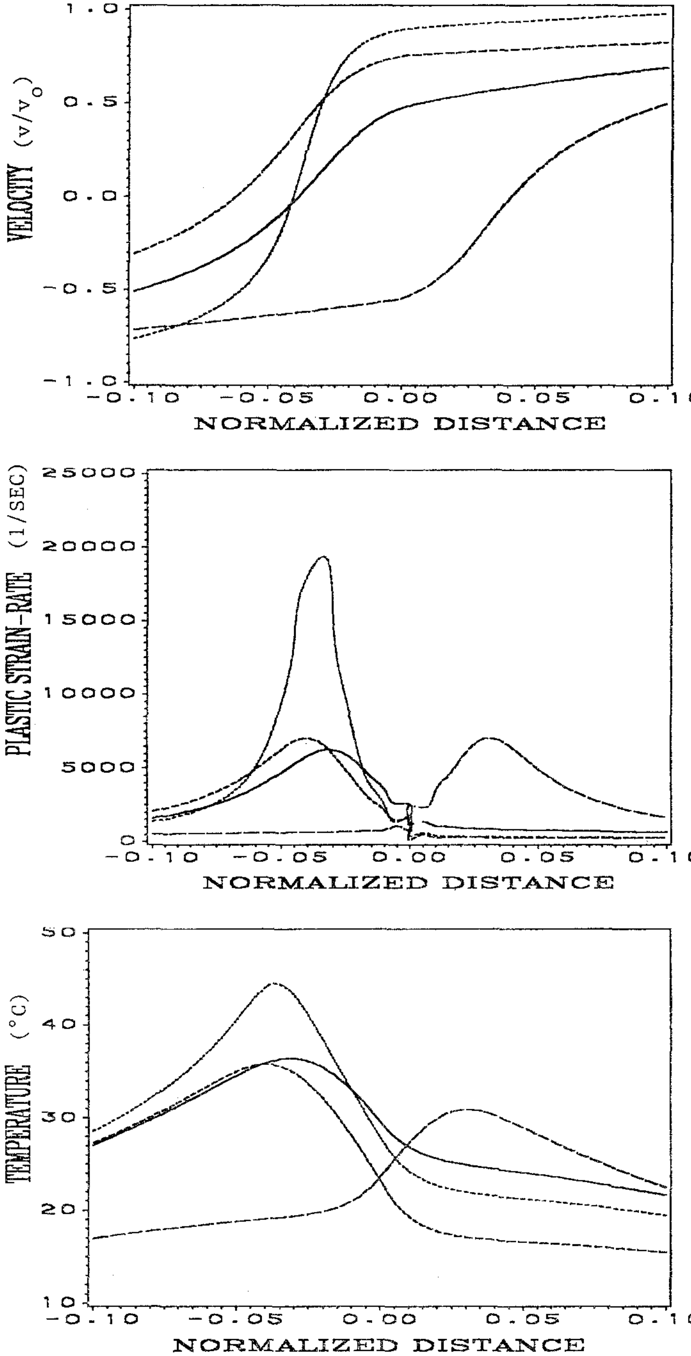

Fig. 3. Distribution of the particle velocity, plastic-strain rate and temperature for $a_2/a_1 = 0.5$, 0.8, 0.9, 1.2 and $\dot{\gamma}_0 = 500\,\mathrm{sec}^{-1}$ at the instants of the localization of the deformation. (------ $a_2/a_1 = 0.5$, $\gamma_{avg} = 0.060$; ······ $a_2/a_1 = 0.8$, $\gamma_{avg} = 0.068$; ——— $a_2/a_1 = 0.9$, $\gamma_{avg} = 0.068$; — — — $a_2/a_1 = 1.2$, $\gamma_{avg} = 0.048$)

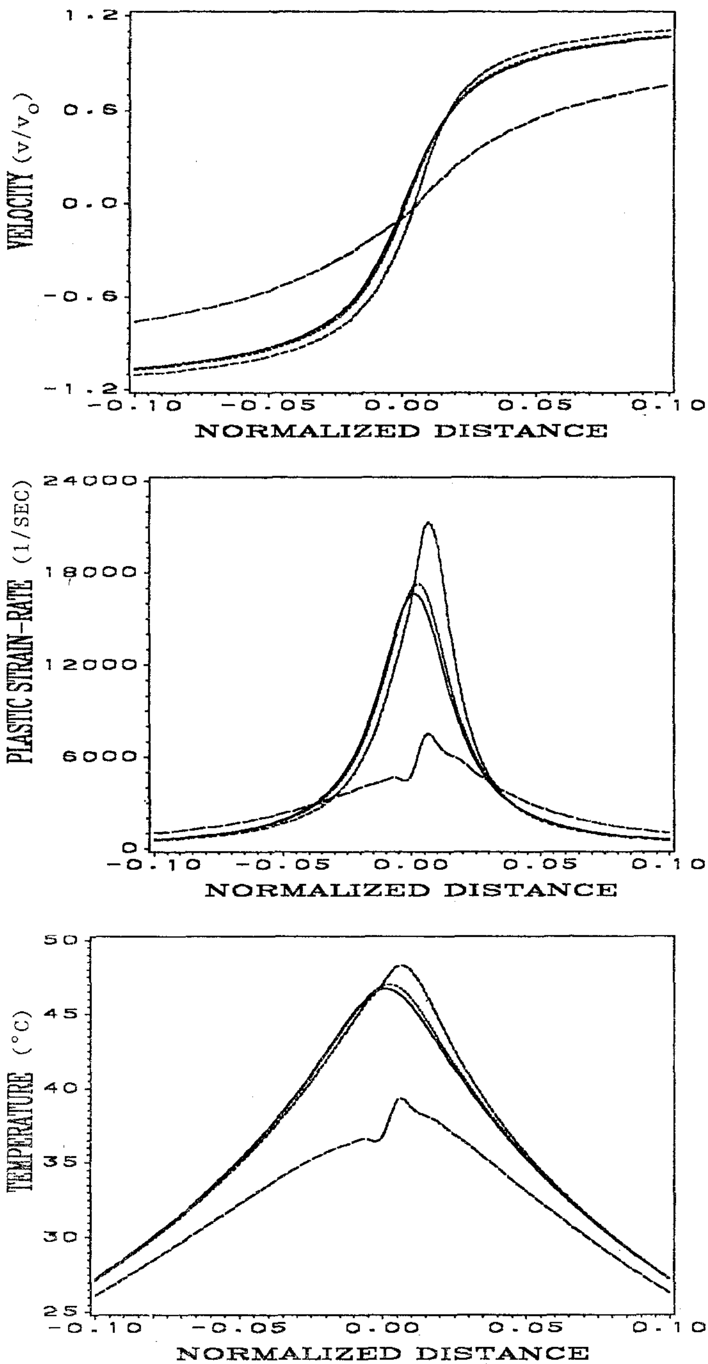

Fig. 4. Distribution of the particle velocity, plastic strain-rate and temperature for $k_2/k_1 = 0.01$, 0.5, 0.8, 0.9 and $\dot{\gamma}_0 = 500\,\text{sec}^{-1}$ at the instants of the localization of the deformation. (———— $k_2/k_1 = 0.01$, $\gamma_{avg} = 0.072$; ------ $k_2/k_1 = 0.50$, $\gamma_{avg} = 0.076$; ...... $k_2/k_1 = 0.80$, $\gamma_{avg} = 0.076$; ——— $k_2/k_1 = 0.90$, $\gamma_{avg} = 0.076$)

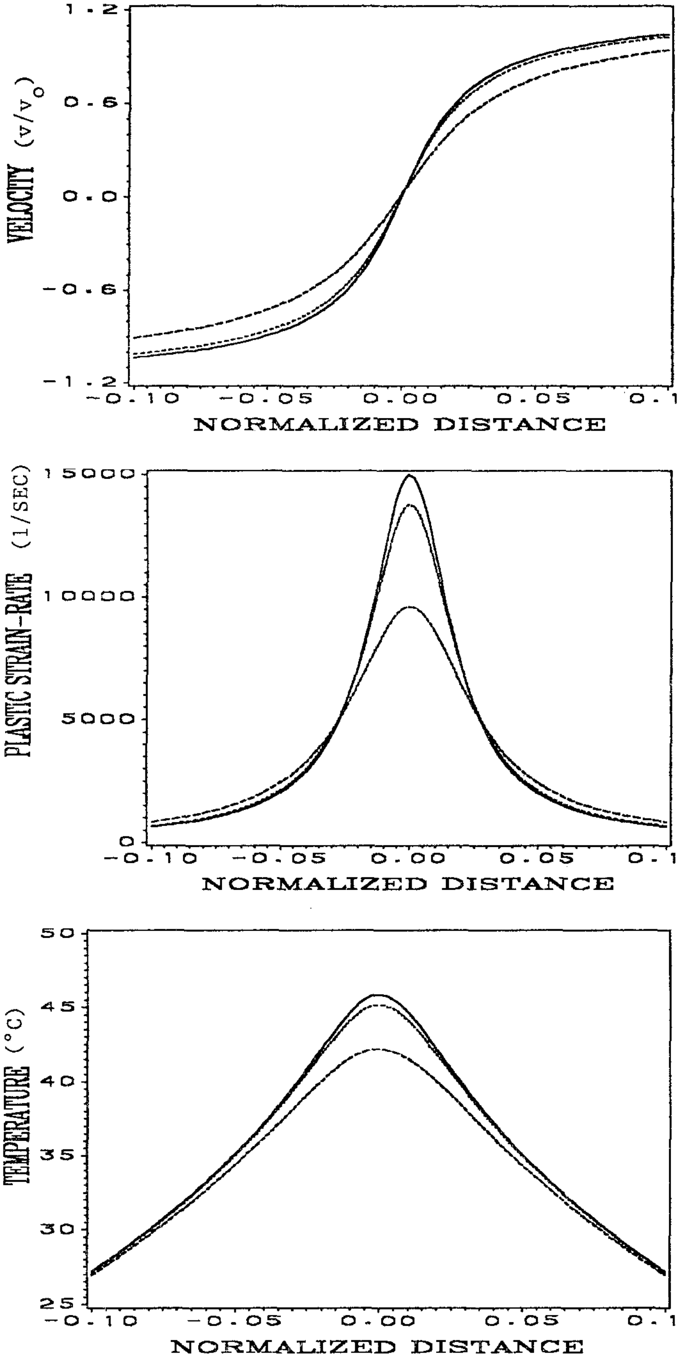

Fig. 5. Distribution of the particle velocity, plastic strain-rate and temperature for $\mu_2/\mu_1 = 0.5$, 0.8 and 0.9 and $\dot{\gamma}_0 = 500\ \text{sec}^{-1}$ at the instants of the localization of the deformation. ($\gamma_{\text{avg}} = 0.076$) (——— $\mu_2/\mu_1 = 0.5$; ...... $\mu_2/\mu_1 = 0.8$; ——— $\mu_2/\mu_1 = 0.9$)

the peak value of the plastic strain-rate occurs at a point where the temperature is maximum rather than where the particle velocity is zero.

In order to see if the mesh size had any effect upon the computed results and in particular the shift in the center of the band away from the center of the specimen where the initial perturbed temperature was maximum, we recomputed results for $a_2/a_1 = 0.8$ but with a finer mesh. In the new mesh (Fig. 1b) the intervals $[-H, -H/10]$, $[-H/10, H/10]$ and $[H/10, H]$ were divided, respectively, into 100, 200, and 100 uniform elements. Thus within the region $[-H/10, H/10]$ the new mesh was five times as fine as the previous one. With this mesh the peak plastic strain rate still occurred at $y/H = -0.035$ and $\gamma_{\text{avg}} = 0.068$. Previous work (Kwon and Batra [27]) on a related problem revealed that the time increment used herein gave results virtually identical to those obtained with $\Delta t = 2.5 \times 10^{-6} v_0/H$. These numerical experiments ensure that the results computed with the uniform mesh of 400 elements and presented herein are reliable.

Figure 4 depicts the particle velocity, plastic strain-rate and the temperature for $k_2/k_1 = 0.01$, 0.5, 0.8, 0.9 and $\dot{\gamma}_{\text{avg}} = 500\ \text{sec}^{-1}$. Note that for all four values of k_2/k_1 the deformation localizes at the same value of the average strain. However, the peak plastic strain-rate and the maximum temperature occur at $y/H = 0.005$, 0.005, 0.0, 0.0 for $k_2/k_1 = 0.01$, 0.5, 0.8, 0.9, respectively. Thus the shift of the center of the band away from the centerline of the specimen is not as pronounced as it was in the previous case. The lower value of the thermal conductivity should result in higher temperatures locally because of the less amount of heat being conducted away from the point. The higher temperature lowers the flow stress which gives rise to higher values of the plastic strain rate since the shear stress becomes uniform soon after the temperature perturbation is introduced. This is evident from the plots for the case $k_2/k_1 = 0.01$. The average strain at which the localization occurs essentially equals that (e.g. 0.0745) for the homogeneous body.

The results plotted in Fig. 5 for $\mu_2/\mu_1 = 0.5$, 0.8, and 0.9 reveal that the deformations of the bimetallic body are symmetrical about the centerline when its two constituents have only differing values of the shear moduli. This is not surprising since, for a homogeneous body, the change in the value of the shear modulus affects little the value of the average strain at which the peak in the shear stress-shear strain curve occurs.

We now study the effect of the applied strain-rate or the prescribed velocity at the top and bottom faces of the specimen. In Fig. 6 is plotted the temperature, plastic strain-rate and the particle velocity for $k_2/k_1 = 0.5$ and $\dot{\gamma}_0 = v_0/H = 500\ \text{sec}^{-1}$, $5{,}000\ \text{sec}^{-1}$, and $50{,}000\ \text{sec}^{-1}$. Whereas for $\dot{\gamma}_0 = 500\ \text{sec}^{-1}$ and $5{,}000\ \text{sec}^{-1}$ the maximum plastic strain-rate occurs where the temperature is maximum such is not the case for $\dot{\gamma}_0 = 50{,}000\ \text{sec}^{-1}$. A possible explanation for this lies in the distribution of the shear stress, plotted in Fig. 7, within the specimen. For $\dot{\gamma}_0 = 500\ \text{sec}^{-1}$ and $5{,}000\ \text{sec}^{-1}$ the shear stress becomes uniform throughout the specimen shortly after the temperature perturbation is introduced

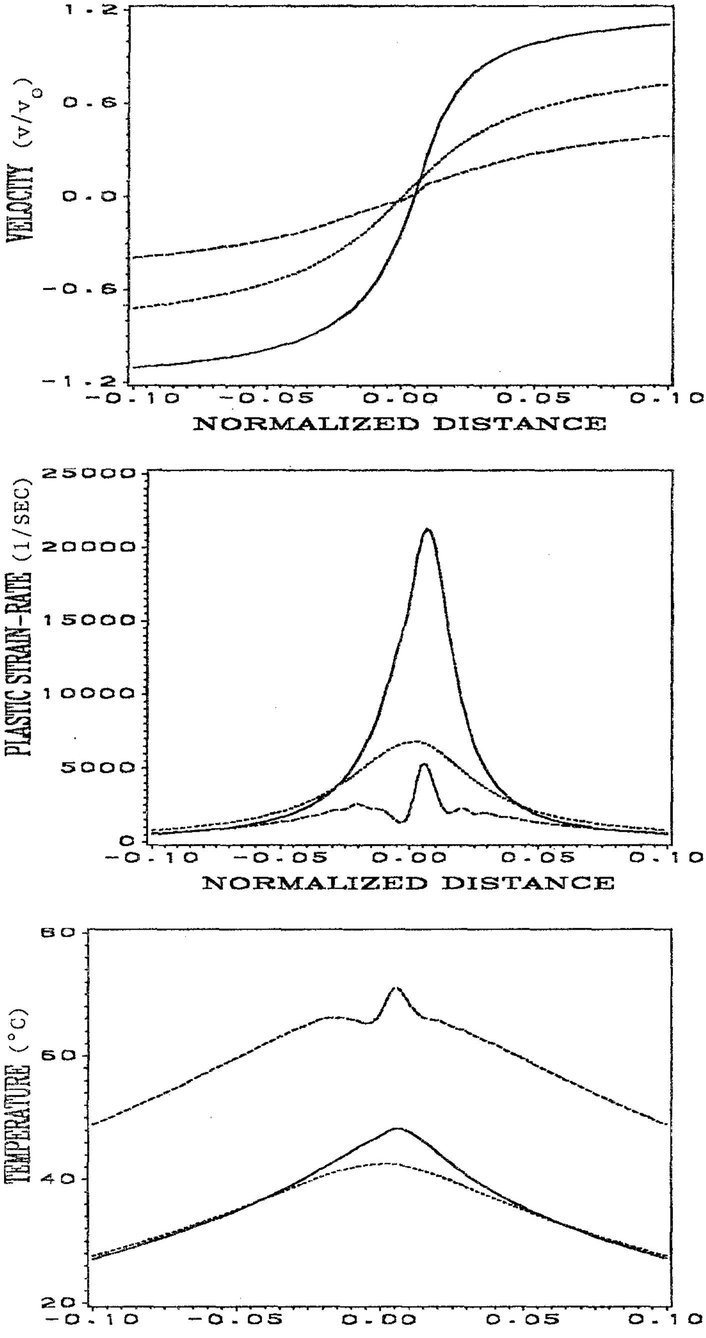

Fig. 6. Distribution of the particle velocity, plastic strain-rate and temperature for $k_2/k_1 = 0.5$ and $\dot{\gamma}_0 = 500\ \text{sec}^{-1}$, $5{,}000\ \text{sec}^{-1}$ and $50{,}000\ \text{sec}^{-1}$ at the instant of the localization of the deformation. (– – – $\dot{\gamma}_0 = 50{,}000\ \text{sec}^{-1}$, $\gamma_{\text{avg}} = 0.208$; ...... $\gamma_0 = 5{,}000\ \text{sec}^{-1}$, $\gamma_{\text{avg}} = 0.076$; ——— $\dot{\gamma}_0 = 500\ \text{sec}^{-1}$, $\gamma_{\text{avg}} = 0.076$)

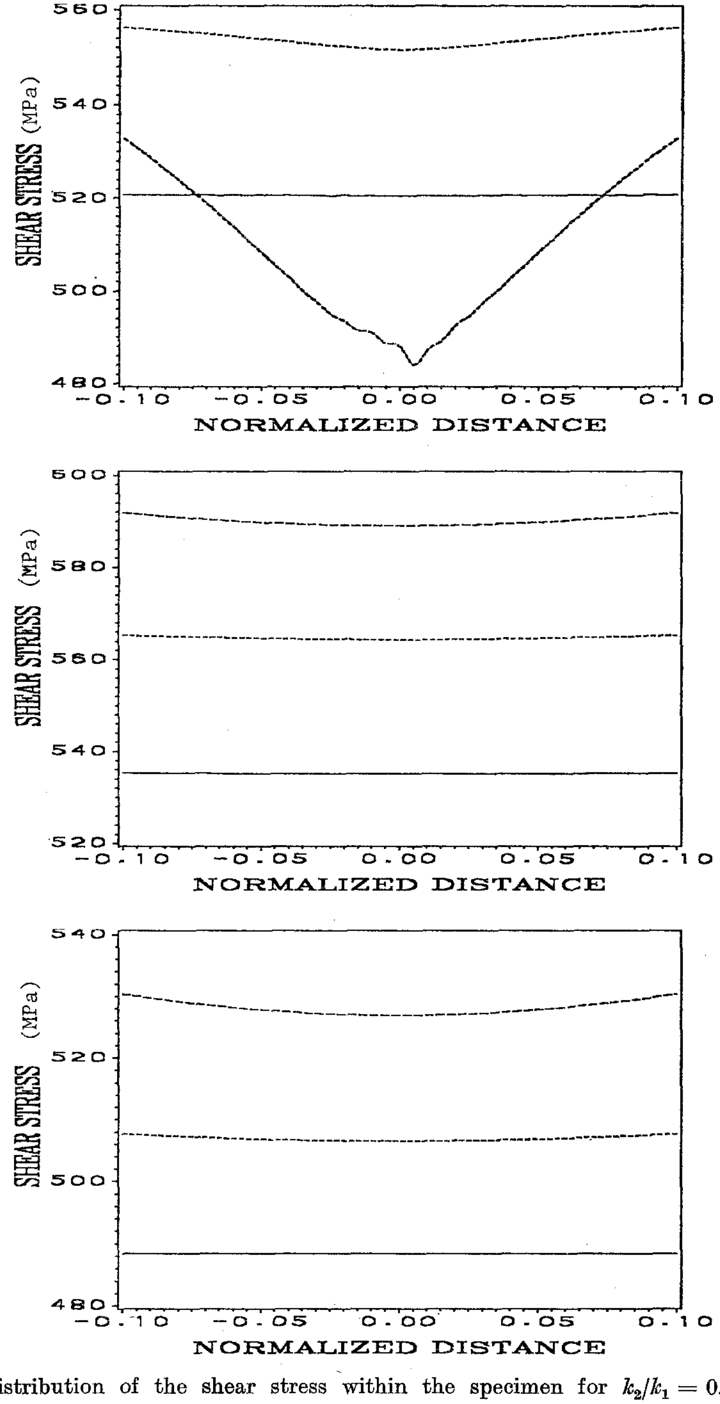

Fig. 7. Distribution of the shear stress within the specimen for $k_2/k_1 = 0.5$, and $\dot{\gamma}_0 = 500\ \text{sec}^{-1}$, $5{,}000\ \text{sec}^{-1}$ and $50{,}000\ \text{sec}^{-1}$ at three different times. (------ $\dot{\gamma}_0 = 50{,}000\ \text{sec}^{-1}$; ······ $\dot{\gamma}_0 = 5{,}000\ \text{sec}^{-1}$; ——— $\dot{\gamma}_0 = 500\ \text{sec}^{-1}$; bottom Fig., $\gamma_{\text{avg}} = 0.004$; middle Fig., $\gamma_{\text{avg}} = 0.064$; top Fig., $\gamma_{\text{avg}} = 0.208$)

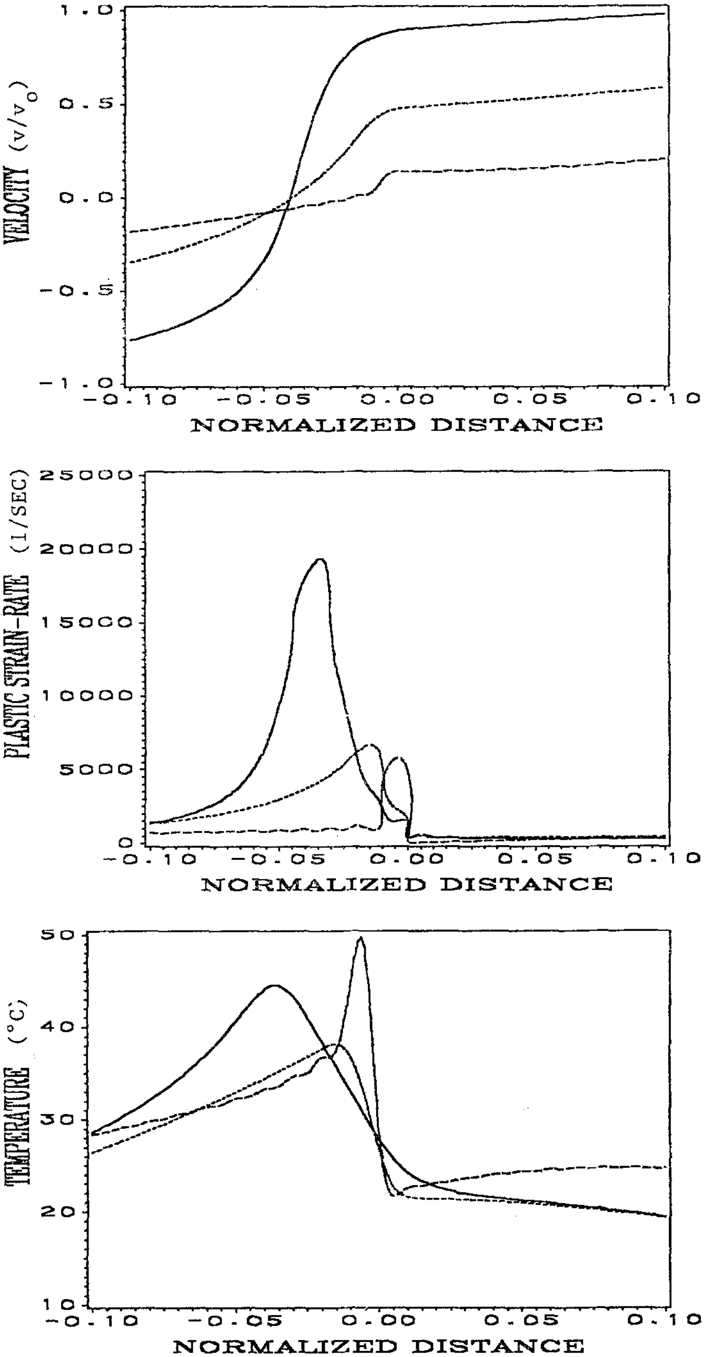

Fig. 8. Distribution of the particle velocity, plastic strain-rate and temperature for $a_2/a_1 = 0.8$ and $\dot{\gamma}_0 = 500\ \text{sec}^{-1}$, $5{,}000\ \text{sec}^{-1}$ and $50{,}000\ \text{sec}^{-1}$ at the instants of localization of the deformation. (– – – $\dot{\gamma}_0 = 50{,}000\ \text{sec}^{-1}$, $\gamma_{\text{avg}} = 0.108$; ······ $\dot{\gamma}_0 = 5{,}000\ \text{sec}^{-1}$, $\gamma_{\text{avg}} = 0.064$; ——— $\dot{\gamma}_0 = 500\ \text{sec}^{-1}$, $\gamma_{\text{avg}} = 0.068$)

and stays so at least through the initiation and some growth of the localization of the deformation. At $\dot{\gamma}_0 = 50{,}000\ \mathrm{sec}^{-1}$ the shear stress becomes uniform after the perturbation is introduced but becomes nonuniform once the deformation starts to localize. This probably is due to the inertia forces playing a significant role at $\dot{\gamma}_0 = 50{,}000\ \mathrm{sec}^{-1}$ and a negligible role at $\dot{\gamma}_0 = 500\ \mathrm{sec}^{-1}$. Batra [22] earlier studied the response of a homogeneous body at $\dot{\gamma}_0 = 50\ \mathrm{sec}^{-1}$, $500\ \mathrm{sec}^{-1}$, $5{,}000\ \mathrm{sec}^{-1}$, and $50{,}000\ \mathrm{sec}^{-1}$ and concluded that the inertia forces become significant at $\dot{\gamma}_0 \geqq 5{,}000\ \mathrm{sec}^{-1}$. Because of the nonuniformity of the shear stress at $\dot{\gamma}_0 = 50{,}000\ \mathrm{sec}^{-1}$ the heat produced due to plastic working is not necessarily maximum where $\dot{\gamma}_p$ is highest thus causing the maximum temperature and the peak plastic strain-rate to occur at different points.

In Fig. 8 we have plotted the particle velocity, plastic strain-rate and the temperature for $a_2/a_1 = 0.8$ and $\dot{\gamma}_0 = 500\ \mathrm{sec}^{-1}$, $5{,}000\ \mathrm{sec}^{-1}$, and $50{,}000\ \mathrm{sec}^{-1}$. For all three values of $\dot{\gamma}_0$ considered the band forms within the material having higher value of the thermal softening coefficient. The peak plastic strain-rate occurs at $y/H = -0.035$, -0.015, and 0.0, respectively, for $\dot{\gamma}_0 = 500\ \mathrm{sec}^{-1}$, $5{,}000\ \mathrm{sec}^{-1}$, and $50{,}000\ \mathrm{sec}^{-1}$. At $\dot{\gamma}_0 = 50{,}000\ \mathrm{sec}^{-1}$ the localization occurs at $\gamma_{\mathrm{avg}} = 0.108$ whereas it occurred at $\gamma_{\mathrm{avg}} = 0.208$ for the homogeneous body [22].

Batra and Kim [28] have used the Gear method to integrate the coupled nonlinear ordinary differential equations obtained by applying the Galerkin approximation to Eqs. (2.1) and (10) and the pertinent boundary conditions. They analyzed the initiation and growth of adiabatic shear bands in a homogeneous body and used the same values of material parameters as those used herein for material 1. Their calculations show that as the deformation localizes the shear stress within the band collapses and an unloading elastic wave emanates outwards from the shear band. When the stress begins to collapse, the temperature at the center of the band equals 79.6% of the presumed melting temperature of the material. It rises to 97% of the melting temperature within 0.9 μsec. Note that it takes 0.807 μsec for the wave to travel to the edge of the specimen. Marchand and Duffy [13] estimated the maximum temperature within the band to be nearly 75% of the melting temperature of the steel tested. Since there was no failure or fracture criterion considered by Batra and Kim, they may have carried their computations too far in time.

As pointed out by Wright and Batra [17], implicit in this problem are two length scales, namely a thermal length $(k/\varrho c \dot{\gamma}_0 H^2)^{1/2}$ and a viscous length $(b/H) \cdot (\varkappa_0/\varrho)^{1/2}$. Here we have varied the thermal length of material 2 relative to that of material 1 in the first set of calculations and of both materials in the second set when the applied strain-rate was changed. Computed results for the monolithic body (Batra [18]) seem to indicate that the thermal length has little effect, if any, on the initiation of the localization of the deformation. Since the calculations in [18] and also herein could not be carried far enough in time, the effect of either the thermal length or the viscous length on the width of the shear band cannot be ascertained.

4. Conclusions

For the bimetallic body the difference in the values of the thermal softening coefficients for the two constituents of the body has a predominant effect on the location of the shear band. The shift in the center of the shear band away from the center of the specimen is more for larger values of a_2/a_1. The band lies completely within the constituent having the higher value of the thermal softening coefficient. The difference in the values of the thermal conductivities shifts the center of the band a little. When one of the constituents has very low thermal conductivity as compared to the other one, plastic strain-rates in it are higher at points equidistant from the center line of the specimen.

The shift in the center of the band decreases with the increase in the applied strain-rate for $a_2/a_1 = 0.8$ but stays the same for $k_2/k_1 = 0.5$. The bands become narrower as the applied strain-rate is increased.

Acknowledgements

This work was supported by the U.S. National Science Foundation grant MSM 8715952 and the U.S. Army Research Office Contract DAAL 03-88-K-0184 to the University of Missouri-Rolla.

References

[1] Zener, C., Hollomon, J. H.: Effect of strain rate on plastic flow of steel. J. Appl. Phys. **14**, 22–32 (1944).

[2] Recht, R. F.: Catastrophic thermoplastic shear. ASME J. Appl. Mech. **31**, 189–193 (1964).

[3] Staker, M. R.: The relation between adiabatic shear instability strain and material properties. Acta Met. **29**, 683–689 (1981).

[4] Clifton, R. J.: Material response to ultra high loading rates. NRC National Material Advisory Board (U.S.) Report **356** (1980).

[5] Clifton, R. J., Molinari, A.: Analytical characterization of shear localization in thermo-viscoplastic materials. J. Appl. Mechs. **54**, 806–812 (1987).

[6] Burns, T. J.: Approximate linear stability analysis of a model of adiabatic shear band formation. Quart. Appl. Math. **43**, 65–83 (1985).

[7] Wright, T. W.: Steady shearing in a viscoplastic solid. J. Mech. Phys. Solids **35**, 269–282 (1987).

[8] Anand, L., Kim, K. H., Shawki, T. G.: Onset of shear localization in viscoplastic solids. Massachusetts Institute of Technology Report, 1986.

[9] Bai, Y. L.: A criterion for thermoplastic shear instability. In: Shock waves and high strain rate phenomenon in metals, pp. 277–283 (Meyers, M. A., Murr, L. E., eds.). New York: Plenum Press (1981).

[10] Coleman, B. D., Hodgdon, M. L.: On shear bands in ductile materials. Arch. Rat'l. Mechs. Anal. **90**, 219–247 (1985).

[11] Moss, G. L.: Shear strain, strain rates and temperature changes in adiabatic shear bands. In: Shock waves and high strain rate phenomenon in metals, pp. 299–312 (Meyer, M. A., Murr, L. E., eds.). New York: Plenum Press 1981.

[12] Costin, L. S., Crisman, E. E., Hawley, R. H., Duffy, J.: On the localization of plastic flow in mild steel tubes under dynamic torsional loading. Inst. Phys. Conf. Ser. No. **47**, 90–100 (1979).

[13] Marchand, A., Duffy, J.: An experimental study of the formation process of adiabatic shear bands in a structural steel. J. Mechs. Phys. Solids **36**, 251–283 (1988).

[14] Clifton, R. J., Duffy, J., Hartley, K. A., Shawki, T. G.: On critical conditions for shear band formation at high strain rates. Scripta Metallurgica **18**, 443 (1984).

[15] Merzer, A. M.: Modeling of adiabatic shear band development from small imperfections. J. Mech. Phys. Sol. **30**, 323–338 (1982).

[16] Wu, F. H., Freund, L. B.: Deformation trapping due to thermoplastic instability in one-dimensional wave propagation. J. Mech. Phys. Sol. **32**, 119–132 (1984).

[17] Wright, T. W., Batra, R. C.: The initiation and growth of adiabatic shear bands. Int. J. Plasticity **1**, 205–212 (1985).

[18] Wright, T. W., Batra, R. C.: Adiabatic shear bands in simple and dipolar plastic materials. In: Proc. IUTAM Symposium on Macro- and Micro-mechanics of High Velocity Deformation and Fracture, pp. 189–201 (Kawata, K., Shioiri, J., eds.) Berlin–Heidelberg–New York: Springer-Verlag 1987.

[19] Wright, T. W., Walter, J. W.: On stress collapse in adiabatic shear bands. J. Mech. Phys. Solids **35**, 701–720 (1987).

[20] Batra, R. C.: The initiation and growth of, and the interaction among, adiabatic shear bands in simple and dipolar materials. Intl. J. Plasticity **3**, 75–89 (1987).

[21] Batra, R. C.: Effect of material parameters on the initiation and growth of adiabatic shear bands. Intl. J. Solids and Structures **23**, 1435–1446 (1987).

[22] Batra, R. C.: Effect of nominal strain-rate on the initiation and growth of adiabatic shear bands. J. Appl. Mechs. **55**, 229–230 (1988).

[23] Rogers, H. C.: Adiabatic plastic deformation. Ann. Rev. Mat. Sci. **9**, 283–311 (1979).

[24] Rogers, H. C.: A review of adiabatic shearing. In: Material behavior under high stress and ultrahigh loading rates, p. 101 (Mexall, J., Weiss, V., eds.). New York: Plenum Press 1983.

[25] Litonski, J.: Plastic flow of a tube under adiabatic torsion. Bulletin de l'Academie Polonaise des Sciences. **25**, 7–14 (1977).

[26] Farren, W. S., Taylor, G. I.: The heat developed during plastic extrusion of metal. Proc. R. Soc. **A 107**, 422–429 (1925).

[27] Kwon, Y. W., Batra, R. C.: Effect of multiple initial imperfections on the initiation and growth of adiabatic shear bands in nonpolar and dipolar materials. Int. J. Engng. Science **26**, 1177–1187 (1988).

[28] Batra, R. C., Kim, C. H.: Adiabatic shear banding in elastic-viscoplastic nonpolar and dipolar materials. Int J. Plasticity (in press)

R. C. Batra and J. W. Kwon
Department of Engineering Mechanics
University of Missouri-Rolla
Rolla, MO 65401-0249
U.S.A.